

EXPERIMENTAL STUDY OF THE FORMATION OF FRACTAL STRUCTURES IN DISPLACEMENT OF IMMISCIBLE FLUIDS USING A HELE-SHAW CELL

B. A. Suleimanov

UDC 532.546

The process of onset of instability of the motion of the interface between immiscible fluids is considered under the predominance of capillary forces. Results of a comparison of experimental and computational data on the effect of the capillary number on the critical length of the perturbation wave are presented.

In spite of the large number of works devoted to the hydrodynamic instability of the displacement of immiscible fluids the problem is still acute. Petroleum engineers first paid attention to this problem in the flooding of oil pools [1-4] and explained it by size inhomogeneity of pores [1]. Of particular interest are works [5, 6]. In [5] it is shown experimentally using a Hele-Shaw cell that instability of the interface between immiscible fluids in displacement of a more viscous fluid by a less viscous one ($\mu_0 = \mu_1/\mu_2 > 1$, μ_1, μ_2 are the viscosities of displacing and displaced fluids, respectively) takes place even in the absence of a porous medium. In [6], on the basis of account for capillary forces, work [5] was supplemented with the conclusion that with relatively small velocities of displacement one can achieve a stable interface (a recalculation for a porous medium is given in [7]).

In [8, 9] the presence of a capillary instability is shown at relatively low rates of filtration, which was also explained by size inhomogeneity of pores. Practically the same result supplemented by numerical models has recently been published [10].

It should be noted that experimental works on displacement of immiscible fluids from relatively homogeneous (microinhomogeneous) hydrophilic porous media give contradictory results when $\mu_0 > 1$. Some researchers believe that instability sets in at supercritical velocities [11-13], and others, in contrast, at subcritical velocities [14, 15], while, lastly, a third group believes that instability can begin at both subcritical and supercritical velocities, i.e., there is an optimum velocity of displacement [8, 16].

Recently, interest in this problem has increased greatly due to the notion of fractal geometry introduced by Mandelbrot for a wide class of surfaces characterized by scale invariance, and a large number of publications have appeared, e.g., [17-20], that are based entirely on classical fluids, right up to those used in experiments [5, 6].

The present work is devoted to a discussion of the stated problems. As regards viscous fingers [21], we used the term "fractal structures" proceeding from the definition of a fractal given by Mandelbrot [17].

To study the process, experiments were conducted on displacement of a Newtonian petroleum by water in a Hele-Shaw cell that consists of two parallel glass plates (length 0.24 m, width 0.14 m) that are at some small distance from each other (the thickness of the gap was $1.2 \cdot 10^{-4}$ m). The packings between the plates limit fluid motion in the cell. There was no packing at one end of the cell and fluid could flow through it, while at the other end there was an opening for fluid intake. To control the dynamics of the displacement process the upper plate was marked every 0.07 m in the direction filtration. Photos were taken of all the structures obtained.

The experiments were conducted according to the following scheme:

a) the horizontally positioned Hele-Shaw cell was vacuum-treated and filled with petroleum of viscosity $12 \cdot 10^{-3}$ Pa·sec;

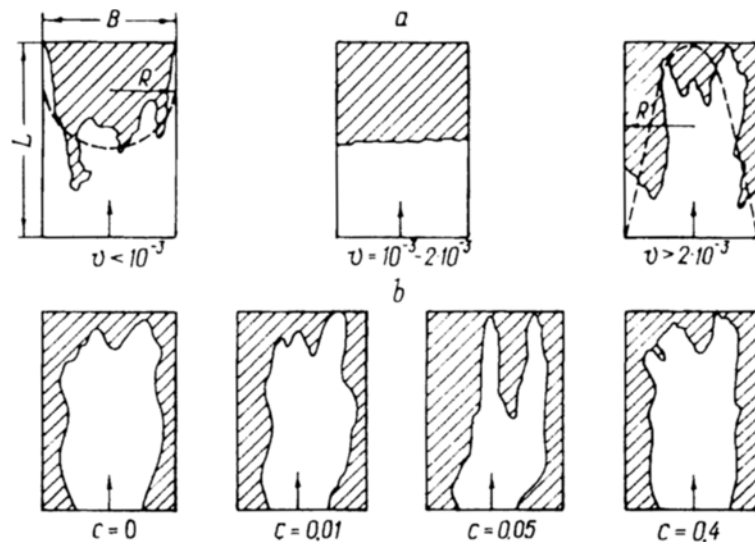


Fig. 1. Fractal structures arising in displacement of petroleum by water (a) and an aqueous solution of SAS (b).

b) water was fed to the cell through the opening, and displacement was performed at different hydrostatic pressures;

c) photographs were taken as the water front reached the marks on the cell.

The experiments were conducted at a temperature of 20°C.

An analysis of the structures obtained at different velocities of front motion (Fig. 1a) showed that at $v = 10^{-3} - 2 \cdot 10^{-3}$ m/sec the front is practically stable and when $v < 10^{-3}$ m/sec and $v > 2 \cdot 10^{-3}$ m/sec the stability of displacement was greatly disturbed, i.e., waterless petroleum output depends nonmonotonically on velocity (Fig. 2a, curve 1) with maximum petroleum output being observed at $v = 10^{-3} - 2 \cdot 10^{-3}$ m/sec. The degree of hydrodynamic instability can be evaluated quantitatively by the Hausdorff–Besikovich dimension d [3]. A calculation of this dimension for the structures obtained showed that $d > 1$ for $v < 10^{-3}$ m/sec and $v > 2 \cdot 10^{-3}$ m/sec, with its maximum value of 1.4 being attained when $v > 2 \cdot 10^{-3}$ m/sec (Fig. 2a, curve 2). According to the results of Nitman, Dakkor, and Stanley (1985) d tends to the value 1.7 for displacement in a plane, and by the data of Feder to the value 2.5 for a three-dimensional case, with these values being independent of the flow velocity and the ratio of the viscosities of the displaced and displacing fluids.

Clear fractal structures can be obtained at subcritical velocities if the Hele–Shaw cell is positioned at an angle, because in this case gravity forces enhance instability.

The dynamics of the displacement process can be explained in the following way. Molecular surface forces at the interface act toward a decrease in the surface area of the interface (i.e., in the direction opposite to the action of hydrodynamic forces), and therefore, when molecular surface forces are predominant over hydrodynamic forces, the velocity distribution on the front is distinguished by the fact that the maximum velocity is observed on the walls and the minimum velocity at the flow center, and the form of the front itself is determined by the radius of curvature (see the dashed line in Fig. 1a for $v < 10^{-3}$ m/sec). When molecular surface forces are balanced by hydrodynamic forces the front becomes almost stable and the picture obtained at $v = 10^{-3} - 2 \cdot 10^{-3}$ m/sec is observed.

When hydrodynamic forces are predominant a front determined by the Poiseuille velocity distribution is obtained (see the dashed line in Fig. 1a for $v > 2 \cdot 10^{-3}$ m/sec). Confirmation of this can be illustrated by the following estimative calculations. Assuming molecular surface forces and hydrodynamic forces to be balanced we determine the critical velocity corresponding to this supposition.

We write the Boussinesq equation

$$v = \frac{b^2}{12\mu} \frac{\Delta P}{L}$$

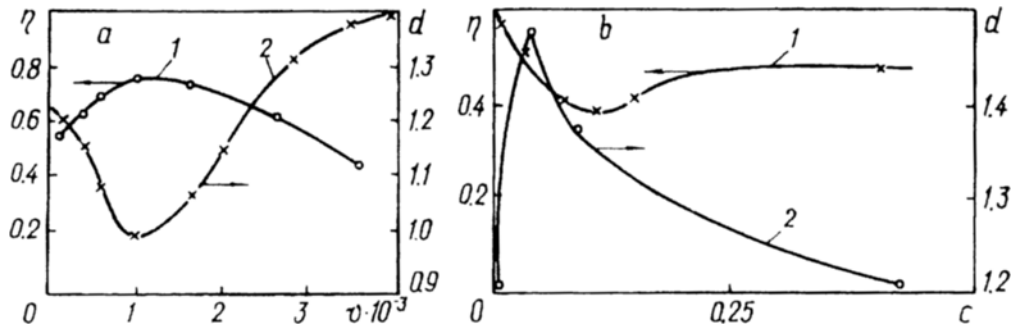


Fig. 2. Dependence of the waterless petroleum output and the Hausdorff-Bezikovich dimension on the flow velocity (m/sec) in displacement of petroleum by water (a, curves 1, 2) and on the SAS concentration (%) in displacement of petroleum by an aqueous solution of SAS (b, curves 1, 2).

and the Laplace equation

$$\Delta P_{\text{cap}} = \frac{2\sigma}{b}.$$

Determining the critical velocity from the condition $\Delta P = \Delta P_{\text{cap}}$, we have

$$v_{\text{cr}} = \frac{\sigma b}{6\mu L}. \quad (1)$$

Substituting the numerical values of the parameters used in the experiments $\sigma = 30 \cdot 10^{-3}$ N/m, $b = 1.2 \cdot 10^{-4}$ m, and $L = 0.24$ m, $\mu = 10^{-3}$ Pa·sec into (1), we find $v_{\text{cr}} \approx 2.5 \cdot 10^{-3}$ m/sec, which corresponds to our considerations.

It is noteworthy that for $v < 10^{-3}$ m/sec, just as for $v > 2 \cdot 10^{-3}$ m/sec, there are dominating directions in the development of viscous fingers; in this case, in spite of the isotropic nature of the cell, the growth of some fingers becomes slower and that of others becomes faster. The structures obtained for $v < 10^{-3}$ m/sec and $v > 2 \cdot 10^{-3}$ m/sec are virtually mirror reflections of each other. Whereas in the first case the viscous finger of the more viscous "lagging" fluid is predominant, since the velocity at the center is a minimum (the "reversed" viscous finger), in the second case the viscous finger of the "advancing" fluid is predominant, since the velocity at the center is a maximum.

The results obtained can be explained by an analysis of the experiments of Gofman (1975), who, using single capillaries, obtained a universal dependence of apparent wettability θ (for wetting fluids) on flow velocity and found that first θ grows according to the law $\theta = w^{1/3}$ (where w is a dimensionless parameter characterizing the velocity of a flow in a capillary) and then it reaches saturation. This dependence shows that at low velocities the meniscus is concave, then it becomes flat, and at relatively high velocities it is convex; this occurs in our case.

We also conducted experiments on the displacement at $\mu_1 = \mu_2$ and $\mu_2 > \mu_1$. Everywhere, in spite of quantitative changes (a range of velocities at which the interface is stable), there was no dependence of waterless petroleum output on a velocity, i.e., the law governing the process is the same as for $\mu_2 < \mu_1$.

Thus, regardless of the ratio of viscosities the front passes through three stages with increase in the velocity: concave, flat, and convex, i.e., it depends only on the molecular surface properties of the fluids. It is obvious that if a less wetting fluid displaces a more wetting one, the front will always be convex, since the capillary and hydrodynamic forces have the same direction (this was probably observed in [5], where air displaced glycerin). It can be shown that similar processes also occur in a hydrophobic cell.

Based on the experiments conducted the dependence of the critical length of the perturbation wave on the capillary number Ca when petroleum is displaced by water (see Fig. 3a, curve 1) was constructed, and a theoretical relation (curve 2) calculated by the formula suggested in [6] was derived for the sake of comparison:

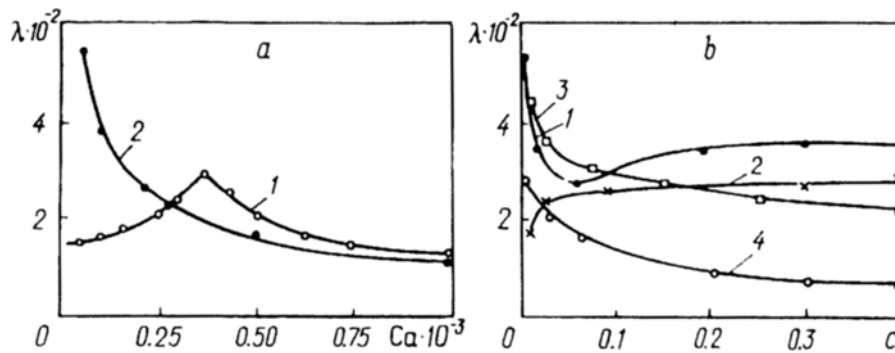


Fig. 3. Experimental and theoretical dependences of the critical wavelength (m) on the capillary number in displacement of petroleum by water (a, curves 1, 2) and on the SAS concentration (%) in displacement of petroleum by an aqueous solution (b, curves 1, 3) and a polymer solution (b, curves 2, 4) of SAS.

$$\lambda = \pi b (Ca)^{-1/2}, \quad Ca = \frac{v(\mu_1 - \mu_2)}{\sigma}, \quad \mu_1 > \mu_2. \quad (2)$$

As is seen from Fig. 3a, in contrast to the theoretical relation the experimental one has a nonmonotonic character: at subcritical velocities (i.e., when $v < 10^{-3}$ m/sec) the critical wavelength is $\lambda \sim Ca^2$ and at supercritical velocities ($v > 2 \cdot 10^{-3}$ m/sec) $\lambda \sim Ca^{-1/2}$.

In a second series of experiments we studied the process of displacement of petroleum by water with addition of SAS (fractal structures are shown in Fig. 1b). Results of the experiments showed that, when SAS is added up to 0.05% inclusive, the quantity of displaced petroleum decreases (see Fig. 2b, curve 1), which is explained by weakening of the restrictive effect of capillary forces.

For $c > 0.05\%$ petroleum output increases. This is explained by the appearance of micelles in the solution, which results in non-Newtonian behavior for the displacer. The obtained dependence of the Hausdorff-Bezikovitch dimension on the SAS concentration in an aqueous solution showed that at $c = 0.05\%$ the fractality of the structure obtained is a maximum and equals 1.45, and at $c = 0.4\%$ it is a minimum and equals 1.2 (see Fig. 2b, curve 2).

An analysis of experimental dependences of the length of the perturbation wave at the front of petroleum displacement on the SAS concentration in an aqueous solution (Fig. 3b, curve 1) and in a 0.02% polymer solution (displacement took place at velocities of a Newtonian flow, Fig. 3b, curve 3), respectively, showed that they have a nonmonotonic character, in contrast to those calculated by formula (2) (see Fig. 3b, curves 2 and 4).

Thus, formula (2), on which practically all studies in this field are based, is applicable only for $\mu_1 > \mu_2$, a flow velocity higher than critical, and Newtonian-fluid flows.

An analysis of the experimental dependence of the position of the displacement front at the point of maximum flowing petroleum output on the hydrostatic pressure (Fig. 4) shows that for $\Delta P < 400$ Pa and $\Delta P > 600$ Pa the maximum flowing petroleum output is attained at the first marks, and then it constantly decreases; this is explained by activation of formation of viscous fingers as the front approaches the outflow.

On the basis of the results obtained one can explain the disconnected character of the experimental results on the displacement of immiscible fluids in a porous medium of various geometries.

The effect of the decrease in waterless petroleum output at relatively low rates of filtration (i.e., when molecular surface forces are predominant) can be explained by the fact that it manifests itself strongly at small ratios of the cell length to its width. This can be illustrated by the following estimates. Assuming that the radius of curvature R of the displacement front is defined as half the cell width B (i.e., complete wetting is assumed) and the cell length is L , we obtain for the coefficient of petroleum output (for the notation see Fig. 1a):

$$\eta = (LB - (\pi R^2/2))/LB = (LB - \pi B^2/8)/LB = 1 - \pi/(8(L/B)).$$

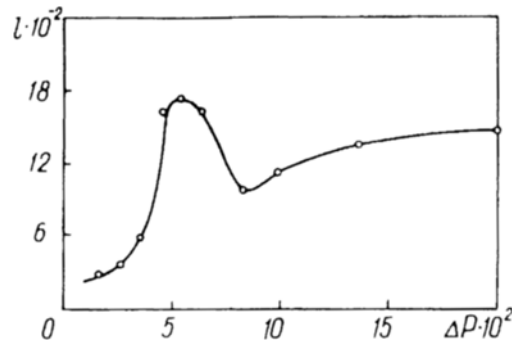


Fig. 4. Dependence of the position of the displacement front at the point of maximum flowing waterless petroleum output (m) on the hydrostatic pressure (Pa).

An analysis of this expression shows that whereas at the minimum length-to-width ratio ($L/B = \delta$) $\delta = 0.5$ (when the interface lies completely within the cell) the petroleum output is 0.2, at $\delta = 10$ it is 0.96, and when $\delta > 10$ it hardly changes.

It can be shown that analogous considerations in the case of an interface determined by the Poiseuille distribution (i.e., when hydrodynamic forces are predominant) lead to the conclusion that in this case the waterless petroleum output is independent of the length-to-width ratio and depends, as shown in [22], only on the ratio of the viscosities of the displacing and displaced fluids, i.e., the effect of the length-to-width ratio plays a determining role precisely when capillary forces are predominant. The laws mentioned are roughly applicable to radial cells as well.

The conclusion obtained is confirmed by experimental studies. Thus, in experiments on cylindrical models of porous media at relatively large δ and with predominance of molecular surface forces the waterless petroleum output is practically independent of the filtration rate [11, 23], and in experiments on relatively short cylindrical cores and gap models [7-9, 24] η decreases with the filtration rate. The conclusion obtained is also confirmed by a number of industrial results [25, 26].

Our data are in good agreement with experimental data of [27, 28]. In [26] the effect of the length of the porous medium (for a constant diameter) on the petroleum output was studied for the following parameters: $\sigma = 30 \cdot 10^{-3}$ N/m; $\mu = 10^{-3}$ Pa·sec, $L = (2-120) \cdot 10^{-2}$ m; $k = 30 \cdot 10^{-12}$ m²; $v = 10$ m/month $\approx 10^{-6}$ m/sec. Calculating the optimum velocity by formula (1) assuming $b = \sqrt{12k} = 2 \cdot 10^{-5}$ m, we obtain $v_{cr} = 5 \cdot 10^{-3} - 8 \cdot 10^{-5}$ m/sec, i.e., the experiment was conducted with predominance of capillary forces. The results of [26] are such that as the length of the model increases from $2 \cdot 10^{-2}$ to $30 \cdot 10^{-2}$ m the petroleum output grows from 25 to 60% for $\mu_0 > 1$, and the kerosene output from 54 to 96% for $\mu_0 \approx 1$, and then it does not change. Meanwhile, from the experimental data obtained by us on cylindrical models of porous media (δ varied from 1 to 30) it was found that in displacement when $\Delta P > \Delta P_{cap}$, an increase in the porous-medium length hardly affects the waterless and final petroleum output.

The results of the studies can be applied to petroleum extraction to analyze macroprocesses of petroleum pool flooding in homogeneous and microinhomogeneous, isotropic pools, i.e., where macroprocesses prevail over microprocesses determined by local fluctuations in the geometry of the pores.

The experiments conducted allow one to make the following conclusions:

- 1) fractal structures form at subcritical velocities even in the absence of a porous medium in a Hele-Shaw cell;
- 2) when capillary forces are predominant, "reverse" fingers of the displaced fluid appear;
- 3) conditions are shown that limit the use of the classical dependence of the critical wavelength on the capillary number;
- 4) it is found that at subcritical velocities the critical length of perturbations is proportional to Ca^2 ;
- 5) the efficiency of the displacement with predominance of capillary forces is strongly dependent on the geometry of the porous medium.

NOTATION

μ_1, μ_2 , viscosity of displaced and displacing fluids, respectively; μ_0 , ratio of viscosities of displaced and displacing fluids; μ , viscosity of water; v , flow velocity; v_{cr} , critical flow velocity; w , dimensionless flow velocity in a capillary; d , Hausdorff–Besikovich dimension; b , gap thickness; L , length of the Hele–Shaw cell; B , width of the Hele–Shaw cell; δ , length-to-width ratio of the cell; R , radius of curvature of the displacement front; λ , critical length of the perturbation wave; ΔP , drop in hydrostatic pressure; ΔP_{cap} , drop in capillary pressure; σ , surface tension; η , petroleum output; k , permeability of the porous medium; c , SAS concentration in the solution; θ , apparent wettability; Ca , capillary number.

REFERENCES

1. F. I. Kotyakhov, *Neft. Khoz.*, No. 6, 31-35 (1950).
2. R. S. Erloger, *Methods of Enhancement of Petroleum Output of Pools* [Russian translation], Moscow, Leningrad, pp. 159-167 (1948).
3. D. N. Dietz, *Proc. Acad. Sci. Amst.*, **56**, 83-90 (1953).
4. R. E. Kidder, *J. Appl. Phys.*, **27**, No. 2, 867-876 (1956).
5. P. G. Saffman and G. J. Taylor, *Proc. Roy. Soc. A*, **245**, No. 1242, 312-319 (1958).
6. R. L. Cnuoke, P. van Meurs, and C. van der Poel, *Trans. Metall. Soc. AIME*, **216**, 188-194 (1959).
7. V. M. Ryzhik and B. E. Kisilenko, *Physicogeological Factors in the Working of Petroleum and Petroleum-Gas-Condensate Fields* [in Russian], Moscow (1969), pp. 82-91.
8. B. E. Kisilenko, *Zh. Prikl. Mekh. Tekh. Fiz.*, No. 6, 194-195 (1961).
9. B. E. Kisilenko, *Izv. Akad. Nauk SSSR, OTN, Mekh. Mashinostr.*, No. 6, 80-84 (1963).
10. R. Lenormand, *Liq. Interfaces: Les Houches Ecole d'Ete Phys. Theor.*, 30 May-24 June, 1988, Sess. 48, Amsterdam etc. (1990), pp. 641-643.
11. D. A. Efros and V. P. Onoprienko, *Tr. VNII*, Issue 12, 331-360 (1958).
12. J. Newcombe, J. Mechee, and M. J. Rzaza, *Trans. AIME*, **204**, 227-241 (1956).
13. A. Kh. Mirzadzhanzade, I. M. Ametov, and A. G. Kovalyov, *Physics of Petroleum and Gas Pools* [in Russian], Moscow (1992).
14. F. I. Kotyakhov, in: *Proc. of a Meeting on the Development of Research Studies in the Field of Secondary Petroleum Production*, Baku (1953), pp. 189-201.
15. J. R. Kyte and L. A. Rapoport, *J. Petrol. Technol.*, No. 10, 64-75 (1958).
16. M. T. Abbasov, N. D. Tairov, D. Sh. Vezirov, et al., *Capillary Effects and Petroleum Output* [in Russian], Baku (1987).
17. J. Feder, *Fractals* [Russian translation], Moscow (1991).
18. I. Nitman, J. Dakkor, and H. Stanley, *Fractals in Physics* [Russian translation], Moscow (1988), pp. 266-282.
19. U. Oxaal, *Phys. Rev. A*, **44**, No. 8, 5038-5051 (1991).
20. U. Oxaal, F. Boger, J. Feder, et al., *Phys. Rev. A*, **44**, No. 10, 6564-6576 (1991).
21. W. F. Engelberts and L. J. Klinkenberg, in: *Petr. Congr. Proc. Third World* (1951), pp. 544-554.
22. A. Kh. Mirzadzhanzade, *Problems of the Hydrodynamics of Viscous-Plastic and Viscous Fluids in Petroleum Production* [in Russian], Baku (1959).
23. S. J. Pirson, *Theory of Petroleum Pools* [Russian translation], Moscow (1961).
24. V. N. Shchelkachev, *Selected Papers* [in Russian], Vol. 2, Moscow (1990).
25. A. I. Mel'nikov, *Neft. Khoz.*, No. 8, 24-26 (1988).
26. B. M. Suchkov, M. B. Kim, and A. A. Vasil'ev, *Neft. Khoz.*, No. 3, 37-40 (1988).
27. I. L. Markhasin, *Physicochemical Mechanics of Petroleum Pools* [in Russian], Moscow (1977).
28. L. S. Melik-Aslanov and V. T. Avanesov, *Tr. AzNII po Dobyche Nefti*, Issue 7, 63-76 (1958).